

University of Groningen

## Highly selective single-component formazanate ferrate(II) catalysts for the conversion of CO<sub>2</sub> into cyclic carbonates

Kamphuis, Aeilke J; Milocco, Francesca; Koiter, Luuk; Pescarmona, Paolo; Otten, Edwin

*Published in:*  
Chemsuschem

*DOI:*  
[10.1002/cssc.201900740](https://doi.org/10.1002/cssc.201900740)

**IMPORTANT NOTE: You are advised to consult the publisher's version (publisher's PDF) if you wish to cite from it. Please check the document version below.**

*Document Version*  
Publisher's PDF, also known as Version of record

*Publication date:*  
2019

[Link to publication in University of Groningen/UMCG research database](#)

*Citation for published version (APA):*

Kamphuis, A. J., Milocco, F., Koiter, L., Pescarmona, P., & Otten, E. (2019). Highly selective single-component formazanate ferrate(II) catalysts for the conversion of CO<sub>2</sub> into cyclic carbonates. *Chemsuschem*, 12(15), 3635-3641. <https://doi.org/10.1002/cssc.201900740>

### Copyright

Other than for strictly personal use, it is not permitted to download or to forward/distribute the text or part of it without the consent of the author(s) and/or copyright holder(s), unless the work is under an open content license (like Creative Commons).

The publication may also be distributed here under the terms of Article 25fa of the Dutch Copyright Act, indicated by the "Taverne" license. More information can be found on the University of Groningen website: <https://www.rug.nl/library/open-access/self-archiving-pure/taverne-amendment>.

### Take-down policy

If you believe that this document breaches copyright please contact us providing details, and we will remove access to the work immediately and investigate your claim.

Downloaded from the University of Groningen/UMCG research database (Pure): <http://www.rug.nl/research/portal>. For technical reasons the number of authors shown on this cover page is limited to 10 maximum.

# Highly Selective Single-Component Formazanate Ferrate(II) Catalysts for the Conversion of CO<sub>2</sub> into Cyclic Carbonates

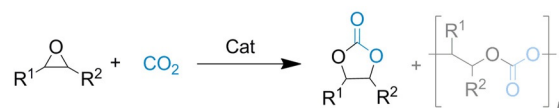
Aeilke J. Kamphuis<sup>+</sup>,<sup>[a]</sup> Francesca Milocco<sup>+</sup>,<sup>[b]</sup> Luuk Koiter,<sup>[b]</sup> Paolo P. Pescarmona,<sup>\*[a]</sup> and Edwin Otten<sup>\*[b]</sup>

The development of new families of active and selective single-component catalysts based on earth-abundant metal is of interest from a sustainable chemistry perspective. In this context, anionic mono(formazanate) iron(II) complexes bearing labile halide ligands, which possess both Lewis acidic and nucleophilic functionalities, have been developed as novel single-component homogeneous catalysts for the reaction of CO<sub>2</sub> with epoxides to produce cyclic carbonates. The influence of

the halide ligand and the electronic properties of the formazanate ligand backbone on the catalytic activity are investigated by employing the iron(II) complexes with and without an additional nucleophile. Very high selectivity is achieved towards the formation of the cyclic carbonate products from various terminal and internal epoxides without the need of a cocatalyst.

## Introduction

The use of carbon dioxide as a C<sub>1</sub> feedstock to produce useful chemicals is highly desirable owing to its low cost and its non-toxic and nonflammable nature.<sup>[1]</sup> One of the biggest challenges associated with the use of CO<sub>2</sub> as a chemical building block consists of overcoming its high thermodynamic stability. This can be achieved by the reaction of CO<sub>2</sub> with compounds that are sufficiently high in free energy to result in exergonic reactions. Examples thereof include the hydrogenation of CO<sub>2</sub> to formic acid or methanol,<sup>[1b,2]</sup> and the 100% atom-efficient reaction of CO<sub>2</sub> with epoxides to produce cyclic carbonates (CCs) or polycarbonates (PCs; Scheme 1).<sup>[3]</sup> Both products are relevant for a number of applications.<sup>[4]</sup> In particular, CCs are used as green solvents, in electrolytes for Li-ion batteries, and as greener alternatives to toxic reagents such as phosgene.<sup>[5]</sup> Another crucial challenge in the fixation of carbon dioxide into CCs and PCs is the development of suitable catalysts, with the purpose of reaching high conversion rates of epoxides and to control the reaction selectivity so that only one of the two products is obtained,<sup>[3]</sup> thus minimizing separation costs. Among the many classes of homogeneous and heterogeneous catalysts that have been studied for the reaction of CO<sub>2</sub> with



**Scheme 1.** Catalyzed reaction of CO<sub>2</sub> with epoxides.

epoxides,<sup>[3,4,6]</sup> the binary catalyst systems involving a Lewis acid (e.g., a metal center) and a nucleophile (e.g., a halide) generally achieve the highest activity and selectivity.<sup>[7]</sup> Several metal complexes have been developed, especially based on Al,<sup>[8]</sup> Zn,<sup>[9]</sup> Co,<sup>[10]</sup> Cr.<sup>[11]</sup> Recently, growing attention has been dedicated to Fe catalysts.<sup>[12,13]</sup> The use of the latter metal is very attractive owing to its abundance, low cost, and relatively low toxicity.<sup>[14]</sup> The Lewis acid center and the nucleophilic species can be provided by two distinct components (e.g., a metal complex and an organic halide) or be incorporated in a single compound (i.e., a bifunctional catalyst). Examples of bifunctional iron-based catalysts include complexes based on Fe<sup>II</sup><sub>[13e,15] or Fe<sup>III</sup><sub>[13a-c,f,16] with multidentate ligands containing N and/or O donor atoms. A limitation of these systems is that, particularly in the case of conversion of internal epoxides, an additional nucleophilic cocatalyst is typically required to achieve high activity and selectivity towards the cyclic carbonate product.</sub></sub>

Here, we report for the first time the use of Fe<sup>II</sup> formazanate complexes as active and selective single-component homogeneous catalysts for the conversion of CO<sub>2</sub> and epoxides into the corresponding cyclic carbonates. In contrast to β-diketiminates, which have been widely used as ligands in metal complexes with application as homogeneous catalysts,<sup>[17]</sup> the structurally related formazanate ligands (based on a NNCNN backbone) have been much less explored.<sup>[18]</sup> Recently, some of us<sup>[19]</sup> and Holland et al.<sup>[20]</sup> reported formazanate iron complexes, including a stoichiometric reaction with CO<sub>2</sub> to give isocya-

[a] A. J. Kamphuis,<sup>+</sup> Prof. P. P. Pescarmona  
Chemical Engineering Group, Engineering and Technology Institute Groningen (ENTEG), University of Groningen  
Nijenborgh 4, 9747 AG Groningen (The Netherlands)  
E-mail: p.p.pescarmona@rug.nl

[b] F. Milocco,<sup>+</sup> L. Koiter, Prof. E. Otten  
Stratingh Institute for Chemistry, University of Groningen  
Nijenborgh 4, 9747 AG Groningen (The Netherlands)  
E-mail: edwin.otten@rug.nl

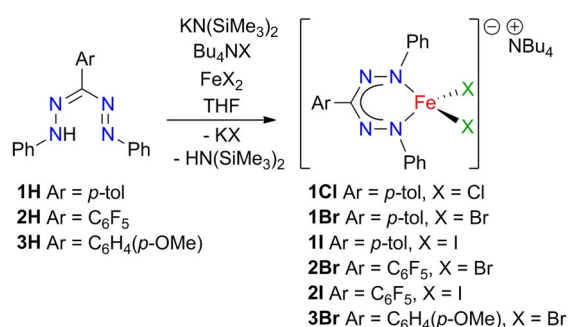
[\*] These authors contributed equally to this work.

Supporting information and the ORCID identification number(s) for the author(s) of this article can be found under:  
<https://doi.org/10.1002/cssc.201900740>.

nate,<sup>[21]</sup> but to the best of our knowledge the application of formazanate iron complexes in catalysis has not been described so far.

## Results and Discussion

The mono(formazanate) ferrate(II) dihalide catalysts,  $[(\text{PhNNC}(\text{Ar})\text{NNPh})\text{FeX}_2]^-$  ( $\text{Ar} = \text{C}_6\text{H}_4(p\text{-Me})$  (**1**),  $\text{C}_6\text{F}_5$  (**2**),  $\text{C}_6\text{H}_4(p\text{-OMe})$  (**3**);  $\text{X} = \text{Cl}, \text{Br}, \text{I}$ ) were synthesized through a modified procedure of a route previously reported by some of us.<sup>[19b]</sup> This new procedure uses a one-pot approach that circumvents the isolation of formazanate alkali metal salts, thus allowing to use ligand substitution patterns that would otherwise lead to decomposition (for example,  $\text{C}_6\text{F}_5$ -substituents engage in nucleophilic aromatic substitution).<sup>[22]</sup> Therefore, simply mixing the formazans **1H–3H** with a tetrabutylammonium halide, a base ( $\text{KN}(\text{SiMe}_3)_2$ ) and  $\text{FeX}_2$  in THF under an inert atmosphere allowed isolation of compounds **1–3** in good yield (60–85%) (Scheme 2).



Scheme 2. Synthesis of compounds 1–3.

Single-crystal X-ray diffraction of the new compounds **2Br/I** and **3Br** (Figure S1; Supporting Information) showed geometries close to tetrahedral (geometry index for four-coordinate complexes  $\tau'_4$  in the range of 0.91–0.93),<sup>[23]</sup> similar to those of the previously reported **1Cl/Br** ( $\tau'_4 = 0.89\text{--}0.90$ ).<sup>[19b]</sup> The Fe–N bond lengths of **2Br/I** and **3Br** (see Table S2) were comparable with those of **1Cl/Br**, in agreement with a high-spin  $\text{Fe}^{\text{II}}$  center ( $S = 2$ ). Compounds **1–3** were characterized in  $[\text{D}_8]\text{THF}$  solution by  $^1\text{H}$  and  $^{19}\text{F}$  NMR spectroscopy (see Supporting Information); broad paramagnetically shifted peaks were observed in the NMR spectra, the number of which was consistent with  $\text{C}_{2v}$  symmetry. The electrochemical behavior of compounds **2Br** and **3Br** was studied by cyclic voltammetry in THF solution (0.1 M  $[\text{Bu}_4\text{N}][\text{PF}_6]$  electrolyte, see Supporting Information). An irreversible oxidation at a peak potential of +0.04 V vs.  $\text{Fc}^{0/+}$  was observed in the anodic scan of **3Br**, which was attributed to the  $\text{Fe}^{\text{II/III}}$  redox couple in analogy to what has been previously observed for **1Br** ( $E_{\text{p,a}} = +0.05$  V vs.  $\text{Fc}^{0/+}$ ).<sup>[19b]</sup> A second oxidation was observed at +0.42 V versus  $\text{Fc}^{0/+}$ , which is probably caused by bromide oxidation.<sup>[24]</sup> The cyclic voltammogram of the  $\text{C}_6\text{F}_5$ -substituted complex **2Br** showed an  $\text{Fe}^{\text{II/III}}$  couple that was shifted to higher potential by more than 100 mV ( $E_{\text{p,a}} = +0.16$  V vs.  $\text{Fc}^{0/+}$ ). The iron oxidation potential can be

used as an indication of the Lewis acidity of the complex, suggesting that the Fe center in **2Br** is a stronger Lewis acid compared with the corresponding sites in **1Br** and **3Br**, as expected if an electron withdrawing group is introduced in the ligand backbone.

The halides in **1Br** were shown to be labile and can be replaced by 4 equivalents of 4-methoxyphenyl isocyanide to give the octahedral cationic complex  $[\text{LFe}(\text{CNC}_6\text{H}_4(p\text{-OMe}))_4][\text{Br}]$ .<sup>[19b]</sup> This feature is promising for the application of this class of complexes as catalysts for the reaction of  $\text{CO}_2$  with epoxides. In this context, the ability of these iron formazanates to activate epoxides was investigated by performing an in situ NMR study. Treatment of a  $[\text{D}_8]\text{THF}$  solution of **1Br** with successive amounts of 1,2-epoxyhexane (1 to 25 equiv.) led to a slight shift in the  $^1\text{H}$  NMR spectrum of the signals of the formazanate moiety (Figure S8), whereas the resonances of the epoxide were hardly affected (Figure S9). Although the changes were relatively minor, we interpreted them as an indication of an equilibrium involving the exchange of bromide with epoxide, albeit shifted towards the starting materials. A similar experiment with pyridine, which is a stronger Lewis base than epoxyhexane, indeed resulted in extensive broadening of the pyridine resonances when 1 equiv. was used, whereas the peaks sharpen when 25 equiv. were added (Figures S10 and S11). These data are consistent with the notion that bromide exchange in **1Br** is facile, but the extent of bromide displacement depends on the nature of the added base. Addition of  $\text{CO}_2$  (1 bar) to the NMR tube containing **1Br** and epoxyhexane (25 equiv.) produced a small amount of cyclic carbonate after standing at room temperature for 2 h. Warming up the sample to  $60^\circ\text{C}$  overnight led to complete conversion of  $\text{CO}_2$  (based on  $^{13}\text{C}$  NMR), together with an increase of the amount of cyclic carbonate (Figure 1).

Encouraged by these initial studies, complexes **1Cl/Br/I** were evaluated as catalysts for the reaction of  $\text{CO}_2$  with 1,2-epoxyhexane in solvent-free conditions at  $90^\circ\text{C}$ , 12 bar  $\text{CO}_2$ . The experiments were run using 0.25 mol% of Fe complex, both with and without the corresponding tetrabutylammonium halide as cocatalyst (Table 1, entries 1–6). Notably, all three formazanate complexes (**1Cl/Br/I**) were active without requiring the addition of a cocatalyst (Table 1, entries 1, 3 and 5). This demonstrated that a halide ligand in these ferrate(II) complexes was sufficiently labile to act as a nucleophile causing ring-opening of the epoxide, resulting in a bifunctional catalytic behavior. A similar mechanism based on a labile metal–halide bond was proposed for (anionic)  $\text{Fe}^{\text{III}}$  catalysts.<sup>[16f]</sup> Virtually complete selectivity (> 99%) towards the cyclic carbonate was observed in all cases. When the corresponding tetrabutylammonium halide was used as cocatalyst in combination with complexes **1Cl/Br/I**, the epoxide conversion was further improved (Table 1, entries 2, 4 and 6). Comparing these results with the activity of the tetrabutylammonium halides under the same conditions but in the absence of iron formazanates (entries 16–18), showed that the presence of the iron complexes led to substantially increased conversion, thus confirming their catalytic activity.

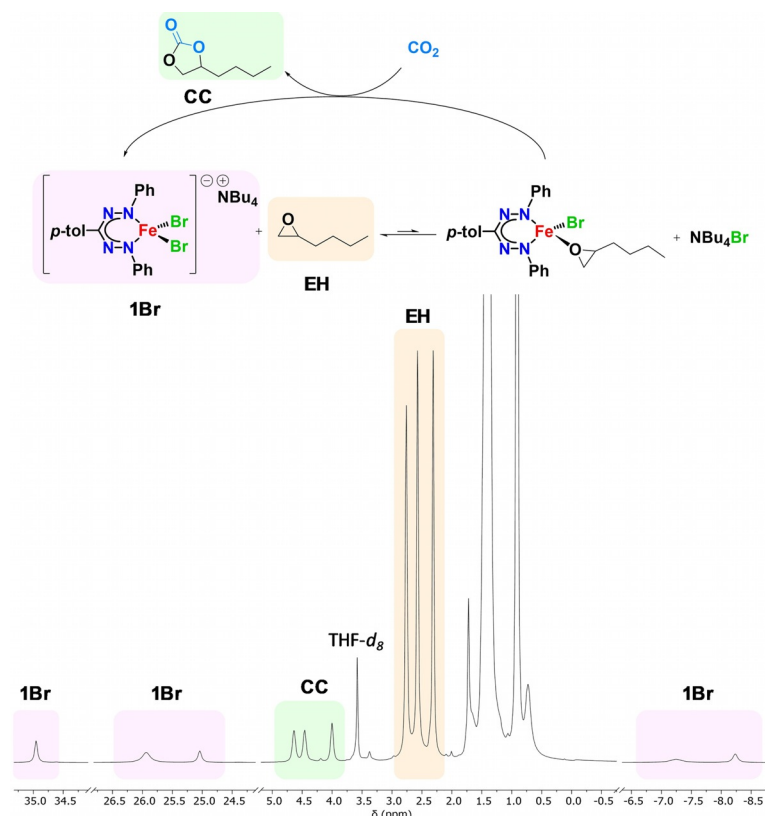


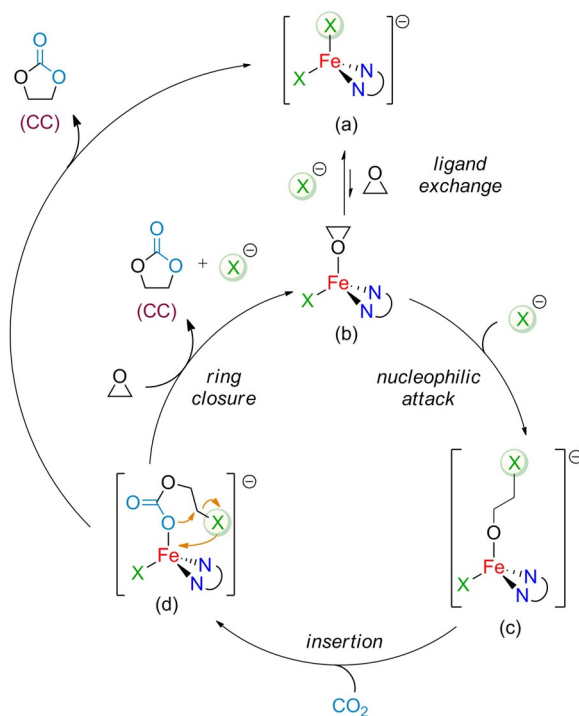
**Figure 1.**  $^1\text{H}$  NMR spectrum of **1Br** + 1,2-epoxyhexane (25 equiv.) +  $\text{CO}_2$  (1 bar) ( $[\text{D}_8]\text{THF}$ , 400 MHz,  $25^\circ\text{C}$ ), selected peaks.

Among the three formazanate complexes (**1Cl/Br/I**), the activity increased in the order of  $\text{X} = \text{Cl}^- < \text{I}^- < \text{Br}^-$ , both in the presence or absence of a cocatalyst. This trend can be understood considering that the overall catalytic activity depends on the nucleophilicity of the halide, its leaving group ability (see Scheme 3 for proposed reaction mechanism) and its interaction with the Lewis acid (i.e., the halide lability from the iron center).<sup>[3c,8c,25]</sup> In the aprotic medium in which the reaction was performed, the nucleophilicity increases in the order of  $\text{I}^- < \text{Br}^- < \text{Cl}^-$ , whereas the leaving group ability decreases in the same order. It can be concluded that in this system bromide provides the best balance between nucleophilicity, leaving group ability, and lability from the iron center, thereby leading to the highest catalytic activity. In addition to studying the effect of the anionic nucleophilic species on the catalytic activity, the influence of the cationic counterpart was also investigated. No significant difference in catalytic activity (34% conversion) was observed when the benchmark reaction was performed with an analogue of complex **1Br** with bis(triphenylphosphine)iminium ( $\text{PPN}^+$ ) as counteranion (equal conditions to Table 1, entry 3).

To further investigate the potential of iron formazanate catalysts in this reaction, the influence of the substituents in the ligand backbone was studied by preparing and testing compounds **2Br**, **2I**, and **3Br**. The electron-withdrawing  $\text{C}_6\text{F}_5$  substituent present in compounds **2Br/I** was expected to lead to a more Lewis-acidic Fe center in comparison with that in com-

plexes **1**, whereas the electron-donating *p*-methoxy group of **3Br** would generate the opposite effect. Comparing the catalytic activity of complex **1Br** (entries 3 and 4) with **2Br** (entries 7 and 8) and **3Br** (entries 10 and 11) shows that all iron complexes are active catalysts, both with and without added cocatalyst, and that both electron-withdrawing and -donating groups have a detrimental effect on activity. The lack of a clear correlation between a single parameter (i.e., the Lewis acidity of the metal center) and the catalytic activity is not surprising given the complex balance between the parameters that determine the activity of the system (such as halide dissociation from the metal center, substrate binding, product release). Complexes **1Br** and **2Br** were also tested using lower loading relative to the epoxide. Under these conditions, a decrease in conversion was observed but a higher turnover number (TON) could be reached (Table S5).

Many homogeneous metal-based catalysts employed in the reaction of  $\text{CO}_2$  with epoxides are air- and moisture-sensitive,<sup>[9a]</sup> requiring drying of the reagents to prevent their deactivation. In the case of the iron formazanate complexes, we investigated the effect of using pre-dried,  $\text{N}_2$ -saturated 1,2-epoxyhexane on the activity of catalyst **1Br** (Table 1, entries 12 and 13). An increase in conversion of approximately 11% was observed in comparison with the test with untreated 1,2-epoxyhexane (entries 3 and 4, respectively). These results indicate that, al-



**Scheme 3.** Proposed mechanism for the reaction of  $\text{CO}_2$  and epoxide catalyzed by  $\text{Fe}^{\text{II}}$  formazanate complexes (**1-3**).

**Table 1.** Reaction of 1,2-epoxyhexane with CO<sub>2</sub> catalyzed by Fe<sup>II</sup> formazanate complexes (1–3).

Entry	Catalyst	Cocatalyst	Conv. [%] <sup>[a]</sup>	TON <sup>[b]</sup>
1	<b>1Cl</b>	–	12	48
2	<b>1Cl</b>	Bu <sub>4</sub> NCl	19	76
3	<b>1Br</b>	–	36	144
4	<b>1Br</b>	Bu <sub>4</sub> NBr	50	200
5	<b>1I</b>	–	21	84
6	<b>1I</b>	Bu <sub>4</sub> NI	28	112
7	<b>2Br</b>	–	24	96
8	<b>2Br</b>	Bu <sub>4</sub> NBr	41	164
9	<b>2I</b>	–	24	96
10	<b>3Br</b>	–	28	112
11	<b>3Br</b>	Bu <sub>4</sub> NBr	39	156
12 <sup>[c]</sup>	<b>1Br</b>	–	47	188
13 <sup>[c]</sup>	<b>1Br</b>	Bu <sub>4</sub> NBr	61	244
14 <sup>[c,d]</sup>	<b>1Br</b>	–	> 99	100
15 <sup>[c,e]</sup>	<b>1Br</b> <sup>[e]</sup>	–	69	–
16	–	Bu <sub>4</sub> NCl	3	–
17	–	Bu <sub>4</sub> NBr	4	–
18	–	Bu <sub>4</sub> NI	5	–

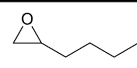
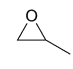
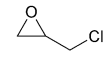
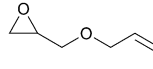
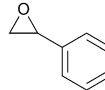
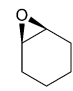
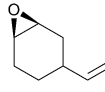
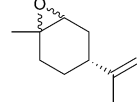
Reaction conditions: 30 mmol epoxide, 3 mmol mesitylene as internal standard, 0.25 mol% Fe complex relative to the epoxide; 0.25 mol% co-catalyst relative to the epoxide (if applicable), 90 °C, 12 bar CO<sub>2</sub> pressure, 2 h. The Fe complexes were fully soluble at room temperature in the reaction mixture. Selectivity towards the cyclic carbonate was > 99% in all cases, as confirmed by <sup>1</sup>H NMR spectroscopy (see Supporting Information). [a] Conversion calculated based on the <sup>1</sup>H NMR signals of the carbonate product and epoxide substrate (see Supporting Information); all runs were conducted in (at least) duplicate, the reported conversion being an average. [b] Turnover number expressed as mol of converted epoxide per mol of catalyst complex. [c] Using anhydrous 1,2-epoxyhexane. [d] 1.00 mol% of complex **1Br** relative to the epoxide. [e] Recycled catalyst from entry 14.

though working with anhydrous reagents is beneficial, the formazanate catalyst is not affected in a major way by adventitious water. This is an important asset, because for practical applications the addition of a drying step would lead to significant undesirable costs.

Of all the formazanate complexes examined, **1Br** showed the highest catalytic activity towards the benchmark reaction of CO<sub>2</sub> with 1,2-epoxyhexane, both with and without an additional nucleophile. Therefore, we chose this complex as a single-component catalyst to expand the scope of the reaction by testing various terminal and internal epoxides (Table 2; for the substrate scope with complex **2Br** see Table S4).

For 1,2-epoxyhexane, the conversion after 18 h (89%) was considerably higher than after 2 h (36%, entry 3 in Table 1), which shows that the formazanate complex **1Br** remained active for an extended period of time. Indeed, the addition of diethyl ether (Et<sub>2</sub>O) after the reaction afforded a precipitate that contained intact **1Br**, as shown by <sup>1</sup>H NMR spectroscopy (Figure S7). This allowed investigating the recyclability of the catalyst. First, a catalytic test with 1.0 mol% catalyst loading was performed, which gave quantitative conversion of 1,2-epoxyhexane after 2 h (Table 1, entry 14). Subsequently, **1Br** was precipitated by the addition of cold Et<sub>2</sub>O/hexane (4:1) under N<sub>2</sub> atmosphere. After removal of the supernatant, the solid was washed with cold Et<sub>2</sub>O, dried, and used without further purifi-

**Table 2.** Substrate scope of the reaction of various terminal and internal epoxides with CO<sub>2</sub> to produce cyclic carbonates, catalyzed by Fe<sup>II</sup> formazanate complex **1Br**.

Entry	Epoxide	Conv. [%] <sup>[a]</sup>	Sel. [%] <sup>[b]</sup>	TON <sup>[c]</sup>
1		89	> 99	356
2 <sup>[f]</sup>		> 99 (97 <sup>[d]</sup> ) 55 <sup>[e]</sup> (43) <sup>[d,e]</sup>	> 99	400 (388 <sup>[d]</sup> ) 1100 <sup>[e]</sup> (860) <sup>[d,e]</sup>
3		89	98	356
4		84	> 99	336
5		70	> 99	280
6		32	98	128
7		18	98	72
8 <sup>[g]</sup>		2	> 99	8

Reaction conditions: 30 mmol epoxide, 3 mmol mesitylene as internal standard, 0.25 mol% of complex **1Br** relative to the epoxide, 90 °C, 12 bar CO<sub>2</sub> pressure, 18 h. [a] Conversion calculated based on the <sup>1</sup>H NMR signals of the carbonate product and epoxide substrate (see Supporting Information). [b] Selectivity towards the cyclic carbonate product determined by FTIR analysis by comparing the C=O stretch signal of the cyclic carbonate and polycarbonate, respectively (see Supporting Information). [c] Turnover number expressed as mol of converted epoxide per mol of catalyst complex. [d] The reported value is based on the yield of propylene carbonate. [e] Catalyst loading: 0.05 mol% of complex **1Br** relative to the epoxide. [f] The small discrepancy between the conversion of propylene oxide and the yield of propylene carbonate is a consequence of the high volatility of propylene oxide, which leads to evaporation of small amounts of epoxide during purging and depressurization of the reactor (see Experimental Section). [g] Reaction conditions: 30 mmol epoxide, 3 mmol mesitylene as internal standard, 1.00 mol% of complex **1Cl** relative to the epoxide, 90 °C, 12 bar CO<sub>2</sub> pressure, 18 h.

cation in a second run. Under identical conditions, the recycled catalyst afforded 69% conversion (Table 1, entry 15). Full catalyst recovery was hampered by its solubility in the carbonate product, and further optimization is required. Nevertheless, these results show that the recovered catalyst retained substantial activity.

Comparing the activity with different substrates, it was observed that **1Br** was especially active in the conversion of terminal epoxides, leading to high conversions (≥ 84%) for reactions of CO<sub>2</sub> with 1,2-epoxyhexane (Table 2, entry 1), epichlorohydrin (entry 3), and allyl glycidyl ether (entry 4). In the case of propylene oxide (entry 2), quantitative conversion was achieved after 18 h with a catalyst loading of 0.25 mol%, accom-

panied by a propylene carbonate yield of 97% (see Table 2, note [f]). Lowering the catalyst loading to 0.05 mol% resulted in a propylene carbonate yield of 43% (entry 2), with a high TON of 860. The conversion of styrene oxide (entry 5) was slightly lower than that of the other terminal epoxides, which can be attributed to the steric hindrance of the aromatic group.

Internal epoxides are typically more difficult to convert owing to steric effects; hence, lower conversions were achieved for the reactions of CO<sub>2</sub> with cyclohexene oxide (entry 6) and vinylcyclohexene oxide (entry 7), whereas only trace amounts of carbonate product were observed with limonene oxide (data not shown). Because it has been reported that smaller nucleophiles are preferred for catalyzing the conversion of highly substituted epoxides,<sup>[26]</sup> **1Cl** was also tested in the reaction of CO<sub>2</sub> with limonene oxide. With a catalyst loading of 1.00 mol%, **1Cl** gave approximately 2% conversion to the corresponding carbonate (entry 8). Although the reaction was very slow, this result demonstrates that formazanate complexes promote the conversion of this challenging substrate even in the absence of a cocatalyst. Interestingly, very high selectivity towards the cyclic carbonate product was also achieved with these cyclohexene-type epoxides, which are known to be prone to copolymerization with CO<sub>2</sub>.<sup>[27]</sup> Typically, in the case of other single-component bifunctional catalysts, the polycarbonate is the major product obtained from the reaction between CO<sub>2</sub> and cyclohexene oxide, and the addition of a separate nucleophile is required to selectively form the cyclic product (see Table S6 for a detailed comparison with other bifunctional iron-based catalysts in the literature).<sup>[13a,c,15c,16a,b]</sup>

## Conclusions

Herein, we have presented the first example of formazanate Fe complexes as homogeneous catalysts for the fixation of CO<sub>2</sub> into cyclic carbonates through reaction with epoxides. The main advantages of these complexes are: (i) their ability to act as single-component catalysts, thus obviating the need for an additional nucleophile; and (ii) their remarkable selectivity towards the cyclic carbonate product, even in the conversion of internal epoxides such as (substituted) cyclohexene oxides, which generally tend to yield polycarbonates. More generally, this work indicates that anionic metal complexes with loosely-bound halide ligands may provide a new entry into single-component transition metal catalysts for the fixation of CO<sub>2</sub> into organic carbonates.

## Experimental Section

### General considerations

The synthesis of the complexes was performed under nitrogen using standard glovebox, Schlenk, and vacuum-line techniques. THF (Aldrich, anhydrous, 99.8%) was dried by percolation over columns of Al<sub>2</sub>O<sub>3</sub> (Fluka); toluene and hexane (Aldrich, anhydrous, 99.8%) were passed over columns of Al<sub>2</sub>O<sub>3</sub> (Fluka), BASF R3-11-supported Cu oxygen scavenger, and molecular sieves (Aldrich, 4 Å). [D<sub>8</sub>]THF (Euriso-top) was vacuum-transferred from Na/K alloy and

stored under nitrogen. The compounds **1H**,<sup>[28]</sup> **3H**,<sup>[29]</sup> PhNNC(C<sub>6</sub>F<sub>5</sub>)H<sup>[30]</sup>, and FeBr<sub>2</sub>(THF)<sub>2</sub><sup>[31]</sup> were synthesized according to literature procedures. Ligand **2H** was prepared according to a slightly adapted version of a literature method<sup>[32]</sup> (see Supporting Information for the detailed description). Aniline (Sigma–Aldrich, 99%), hydrochloric acid (Boom B.V., 37–38%), glacial acetic acid (Imisure, 100%), sodium hydroxide (pellets, Acros), sodium nitrite (Sigma–Aldrich), acetone (Boom B.V., technical grade), methanol (Boom B.V., technical grade), hexane (Boom B.V., technical grade), CDCl<sub>3</sub> (Euriso-top), tetrabutylammonium bromide (Sigma–Aldrich, 99%), tetrabutylammonium chloride (Sigma–Aldrich, 99%), tetrabutylammonium iodide (Sigma–Aldrich, 98%), FeI<sub>2</sub> (Alfa Aesar, anhydrous, 97%), and potassium bis(trimethylsilyl)amide (Sigma–Aldrich, 95%) were used as received. KH (Sigma–Aldrich, 30 wt% dispersion in mineral oil) was washed several times with hexane to remove the mineral oil and subsequently dried in vacuo to obtain a fine powder. NMR spectra were recorded on a Varian Oxford 300 MHz, Varian Mercury 400 MHz, Inova 500 MHz, or Bruker 600 MHz spectrometer. The <sup>1</sup>H and <sup>13</sup>C NMR spectra were referenced internally using the residual solvent resonances and reported in ppm relative to TMS (0 ppm). FTIR spectra were recorded using a Shimadzu IR tracer-100 equipped with an ATR sample unit with a frequency range of 4000–600 cm<sup>-1</sup>, a resolution of 4 cm<sup>-1</sup>, and 64 scans. Cyclic voltammetry was performed using a three-electrode setup with a silver wire pseudo-reference electrode and a platinum disk working electrode (CHI102, CH Instruments; diameter = 2 mm). The platinum working electrode was polished before the experiment using an alumina slurry (0.05 μm), rinsed with distilled water, and subjected to brief ultrasonication to remove any adhered alumina microparticles. The electrodes were then dried in an oven at 75 °C overnight to remove any residual traces of water. The CV data were calibrated by adding decamethylferrocene as a THF solution at the end of the experiments. There was no indication that the addition of decamethylferrocene influenced the electrochemical behavior of the products. All electrochemical measurements were performed at ambient temperatures under an inert N<sub>2</sub> atmosphere in THF containing 0.1 M [Bu<sub>4</sub>N][PF<sub>6</sub>] as the supporting electrolyte. Data were recorded with *Autolab NOVA* software (version 2.1–2). UV/Vis spectra were recorded in a THF solution (≈ 10<sup>-5</sup> M) using an Agilent Cary 8454 UV/Vis spectrophotometer.

### Synthesis of the iron complexes

**[Bu<sub>4</sub>N][(PhNNC(*p*-tol)NNPh)FeCl<sub>2</sub>] (1Cl)**: To a solution of **1H** (276.3 mg, 1.0 equiv., 0.88 mmol) in THF (20 mL), tetrabutylammonium chloride (244.3 mg, 1.0 equiv., 0.88 mmol), potassium bis(trimethylsilyl)amide (203.0 mg, 1.1 equiv., 0.97 mmol), and FeCl<sub>2</sub> (111.4 mg, 1.0 equiv., 0.88 mmol) were added as solids. The dark purple mixture was stirred for 3 d, after which the volatiles were removed in vacuo. The product was extracted in THF (2 × 6 mL) and slow diffusion of hexane into the THF solution afforded dark purple crystals, which were filtered and washed with toluene and hexane to give **1Br** (473.8 mg, 0.69 mmol, 79% yield). The <sup>1</sup>H NMR spectrum was in agreement with the literature.<sup>[19b]</sup>

**[Bu<sub>4</sub>N][(PhNNC(*p*-tol)NNPh)FeBr<sub>2</sub>] (1Br)**: To a solution of **1H** (572.2 mg, 1.0 equiv., 1.82 mmol) in THF (25 mL), tetrabutylammonium bromide (586.7 mg, 1.0 equiv., 1.82 mmol), potassium hydride (89.0 mg, 1.2 equiv., 2.20 mmol), and FeBr<sub>2</sub>(THF)<sub>2</sub> (655.0 mg, 1.0 equiv., 1.82 mmol) were added as solids. The dark purple mixture was stirred for 3 d, after which the volatiles were removed in vacuo. The product was extracted in THF (2 × 25 mL) and slow diffusion of hexane into the THF solution afforded dark purple crystals, which were filtered and washed with toluene and hexane to

give **1Br** (1024.2 mg, 1.33 mmol, 73 % yield). The  $^1\text{H}$  NMR spectrum was in agreement with the literature.<sup>[19b]</sup>

**[Bu<sub>4</sub>N][(PhNNC(*p*-tol)NNPh)FeI<sub>2</sub>] (1I):**<sup>[20b]</sup> To a solution of **1H** (565.9 mg, 1.0 equiv., 1.80 mmol) in THF (25 mL), tetrabutylammonium iodide (664.7 mg, 1.0 equiv., 1.80 mmol), potassium hydride (87.4 mg, 1.2 equiv., 2.20 mmol), and FeI<sub>2</sub> (556.1 mg, 1.0 equiv., 1.80 mmol) were added as solids. After stirring at RT for 1 day, the volatiles were removed in vacuo. The product was extracted in THF (2×20 mL) and slow diffusion of hexane into the THF solution afforded a dark purple powder, which was filtered and washed with toluene and hexane to give **1I** (826.6 mg, 1.14 mmol, 63 % yield).  $^1\text{H}$  NMR (400 MHz, [D<sub>8</sub>]THF, 25 °C):  $\delta$  = 36.34 (3H, *p*-tol CH<sub>3</sub>), 30.07 (4H, Ph *m*-CH), 25.15 (2H, *p*-tol *m*-CH), 2.73 (8H, NBu<sub>4</sub><sup>+</sup>, CH<sub>2</sub>), 2.47 (8H, NBu<sub>4</sub><sup>+</sup>, CH<sub>2</sub>), 1.37 (8H, NBu<sub>4</sub><sup>+</sup>, CH<sub>2</sub>), 0.83 (12H, NBu<sub>4</sub><sup>+</sup>, CH<sub>3</sub>), -8.79 (2H, Ph *p*-CH), -9.42 (2H, *p*-tol *o*-CH), -24.49 ppm (4H, Ph *o*-CH). Anal. calcd for C<sub>35</sub>H<sub>46</sub>N<sub>5</sub>I<sub>2</sub>Fe: C 49.96, H 6.17, N 8.09; found: C 50.58, H 6.81, N 7.13.

**[Bu<sub>4</sub>N][(PhNNC(C<sub>6</sub>F<sub>5</sub>)NNPh)FeBr<sub>2</sub>] (2Br):** To a solution of **2H** (858.7 mg, 1.0 equiv., 2.20 mmol) in THF (30 mL), tetrabutylammonium bromide (695.0 mg, 0.98 equiv., 2.16 mmol), potassium bis(trimethylsilyl)amide (478.8 mg, 1.1 equiv., 2.40 mmol), and FeBr<sub>2</sub>·(THF)<sub>2</sub> (791.7 mg, 1.0 equiv., 2.20 mmol) were added as solids. The reaction mixture was stirred for 3 d, after which the volatiles were removed in vacuo. The product was washed with toluene (20 mL) and subsequently extracted in THF (2×15 mL). Slow diffusion of hexane into the orange-brown THF solution at RT afforded a dark brown solid, which was filtered and washed with toluene and hexane to give **2Br** (1266.0 mg, 1.49 mmol, 69 % yield).  $^1\text{H}$  NMR (400 MHz, [D<sub>8</sub>]THF, 25 °C):  $\delta$  = 23.76 (4H, Ph *m*-CH), 4.44 (8H, NBu<sub>4</sub><sup>+</sup>, CH<sub>2</sub>), 2.95 (8H, NBu<sub>4</sub><sup>+</sup>, CH<sub>2</sub>), 2.19 (8H, NBu<sub>4</sub><sup>+</sup>, CH<sub>2</sub>), 1.31 (12H, NBu<sub>4</sub><sup>+</sup>, CH<sub>3</sub>), -5.54 (2H, Ph *p*-CH), -16.70 ppm (br, 4H, Ph *o*-CH).  $^{19}\text{F}$ -NMR (376 MHz, [D<sub>8</sub>]THF, 25 °C):  $\delta$  = -125.12 (1F, C<sub>6</sub>F<sub>5</sub> *p*-CF), -130.24 (2F, C<sub>6</sub>F<sub>5</sub> CF), -157.72 ppm (2F, C<sub>6</sub>F<sub>5</sub> CF). Anal. calcd for C<sub>35</sub>H<sub>46</sub>N<sub>5</sub>Br<sub>2</sub>Fe: C 49.61, H 5.47, N 8.26; found: C 49.36, H 5.53, N 7.86.

**[Bu<sub>4</sub>N][(PhNNC(C<sub>6</sub>F<sub>5</sub>)NNPh)FeI<sub>2</sub>] (2I):** To a solution of **2H** (267.4 mg, 1.0 equiv., 0.69 mmol) in THF (15 mL), tetrabutylammonium iodide (253.0 mg, 1.0 equiv., 0.69 mmol), potassium bis(trimethylsilyl)amide (158.2 mg, 1.1 equiv., 0.75 mmol), and FeI<sub>2</sub> (218.7 mg, 1.0 equiv., 0.69 mmol) were added as solids. After stirring the reaction mixture for 3 d, the volatiles were removed in vacuo. The product was washed with hexane and toluene and subsequently extracted in THF. Slow diffusion of hexane into the orange-brown THF solution at RT afforded a dark brown solid, which was filtered and washed with toluene and hexane to give **2I** (393.4 mg, 0.42 mmol, 61 % yield).  $^1\text{H}$  NMR (400 MHz, [D<sub>8</sub>]THF, 25 °C):  $\delta$  = 27.98 (4H, Ph *m*-CH), 2.26 (8H, NBu<sub>4</sub><sup>+</sup>, CH<sub>2</sub>), 1.94 (8H, NBu<sub>4</sub><sup>+</sup>, CH<sub>2</sub>), 1.72 (8H, NBu<sub>4</sub><sup>+</sup>, CH<sub>2</sub>), 1.22 (12H, NBu<sub>4</sub><sup>+</sup>, CH<sub>3</sub>), -5.02 ppm (2H, Ph *p*-CH). \*  $^{19}\text{F}$ -NMR (376 MHz, [D<sub>8</sub>]THF, 25 °C):  $\delta$  = -123.58 (1F, C<sub>6</sub>F<sub>5</sub> *p*-CF), -128.89 (2F, C<sub>6</sub>F<sub>5</sub> CF), -158.55 ppm (2F, C<sub>6</sub>F<sub>5</sub> CF). Anal. calcd for C<sub>35</sub>H<sub>46</sub>N<sub>5</sub>I<sub>2</sub>Fe: C 44.65, H 4.93, N 7.44; found: C 44.42, H 4.88, N 7.39. \*The peak of Ph *o*-CH was not visible owing to paramagnetic line broadening.

**[Bu<sub>4</sub>N][(PhNNC(C<sub>6</sub>H<sub>4</sub>(*p*-OME)NNPh)FeBr<sub>2</sub>] (3Br):** To a solution of **3H** (660.8 mg, 1.0 equiv., 2.00 mmol) in THF (30 mL), tetrabutylammonium bromide (644.7 mg, 1.0 equiv., 2.00 mmol), potassium bis(trimethylsilyl)amide (462.0 mg, 1.1 equiv., 2.20 mmol), and FeBr<sub>2</sub>·(THF)<sub>2</sub> (719.7 mg, 1.0 equiv., 2.00 mmol) were added as solids. The reaction mixture was stirred for 3 d, after which the volatiles were removed in vacuo. The product was extracted in THF (2×20 mL) and slow diffusion of hexane into the fuchsia THF solution at RT afforded a dark purple solid, which was filtered and washed with toluene and hexane to give **3Br** (1342.9 mg, 1.71 mmol, 85 % yield).  $^1\text{H}$  NMR (400 MHz, [D<sub>8</sub>]THF, 25 °C):  $\delta$  = 26.24 (4H, Ph *m*-CH),

24.11 (2H, C<sub>6</sub>H<sub>4</sub>OCH<sub>3</sub> *m*-CH), 9.38 (3H, C<sub>6</sub>H<sub>4</sub>OCH<sub>3</sub> *p*-OCH<sub>3</sub>), 2.82 (8H, NBu<sub>4</sub><sup>+</sup> CH<sub>2</sub>), 1.30–2.00 (16H, NBu<sub>4</sub><sup>+</sup> CH<sub>2</sub>), 0.91 (12H, NBu<sub>4</sub><sup>+</sup> CH<sub>3</sub>), -7.27 (2H, C<sub>6</sub>H<sub>4</sub>OCH<sub>3</sub> *o*-CH), -8.93 (2H, Ph *p*-CH), -19.76 ppm (br, 4H, Ph *o*-CH). Anal. calcd for C<sub>36</sub>H<sub>53</sub>N<sub>5</sub>OBr<sub>2</sub>Fe: C 54.91, H 6.79, N 8.89; found: C 54.79, H 6.43, N 8.61.

### Catalytic tests

The catalytic experiments were conducted in a high-throughput CO<sub>2</sub> reactor unit constructed by ILS-Integrated Lab Solutions GmbH. This CO<sub>2</sub> reactor unit consisted of: (a) a 10-reactors block that allows 10 reactions to be performed simultaneously in individually stirred batch reactors (84 mL volume each, 30 mm internal diameter); and (b) a single batch reactor with the same dimensions and equipped with a borosilicate glass window to allow visualization of the phase behavior within the reactor. The unit can operate in a temperature range of 20–200 °C and a pressure range of 1–200 bar. For each test, 30.0 mmol epoxide, 3.0 mmol mesitylene as internal standard and the appropriate amounts of catalyst and co-catalyst (when used) were weighed into a glass vial (46 mL volume, 30 mm external diameter) equipped with a magnetic stirring bar and a screw cap containing a silicone/PTFE septum. The glass vials were then transferred into the 10-reactors block and each septum was pierced with two thin syringe needles to allow gas to flow in and out of the vials. The reactors block was subsequently closed. The parallel batch reactors were first purged 3 times with 5 bar N<sub>2</sub>, after which they were pressurized to 10 bar CO<sub>2</sub>. After waiting for 10 min, the reactors were depressurized to atmospheric pressure to prevent damage to the Viton O-rings. After atmospheric pressure was reached, another 10 min were waited. Next, the reactors were pressurized with 10 bar CO<sub>2</sub>. After reaching this pressure, the reactors block was heated to 90 °C, which resulted in a final pressure of approximately 12 bar in each batch reactor. The process of purging, pressurizing, and heating the reactors block took approximately 1 h. The start of the reaction was defined as the moment at which the magnetic stirring was switched on, after reaching the desired reaction temperature and pressure. The reactions were performed at 900 rpm stirring speed for either 2 or 18 h. At the end of the reaction, the magnetic stirring and the reactor heating were switched off and the water-cooling system was turned on to cool down the reactors block. Upon reaching room temperature, the reactors were depressurized. The process of cooling down and depressurizing the reactors block took approximately 45 min. After reaching atmospheric pressure, the reactors block was opened, and the vials were removed. Small aliquots of each sample were used for  $^1\text{H}$  NMR and FTIR analyses.

The recycling tests were conducted in the visualization reactor of the high-throughput CO<sub>2</sub> reactor unit at 90 °C, 12 bar CO<sub>2</sub> pressure, 2 h, following the same catalytic testing procedure reported above. 1,2-Epoxyhexane and mesitylene were previously dried on molecular sieves and degassed under N<sub>2</sub>. For the first run, 30.0 mmol epoxide, 3.0 mmol mesitylene as internal standard, and 1.0 mol% of **1Br** relative to the epoxide were employed. After the reaction, cold Et<sub>2</sub>O and hexane (in a volume ratio 4:1) were added under N<sub>2</sub>. The fuchsia-colored mixture was stirred until a precipitate formed. Then, the stirring was stopped, and the supernatant was decanted. The obtained solid was washed with cold Et<sub>2</sub>O and dried to obtain a dark purple solid, which was directly used in the second catalytic run without any further purification. For the second run, 30.0 mmol epoxide and 3.0 mmol mesitylene were added to the recovered catalyst and the recycling test was performed under the same conditions as in the first run.

The description of the synthesis of ligand **2H**, the characterization of the complexes and the <sup>1</sup>H NMR and FTIR spectra used to quantify the conversions and yields of the catalytic tests are provided in the Supporting Information. CCDC 1889271, 1889272 and 1889273 contain the supplementary crystallographic data for this paper. These data can be obtained free of charge from The Cambridge Crystallographic Data Centre.

## Acknowledgements

We are thankful for the financial support of NWO for a Vidi grant to E.O. We acknowledge Yasser Alassmy for scientific discussion and help in the recycling tests.

## Conflict of interest

The authors declare no conflict of interest.

**Keywords:** CO<sub>2</sub> fixation • cyclic carbonates • formazanate ligands • homogeneous catalysis • iron

- [1] a) Q. Liu, L. Wu, R. Jackstell, M. Beller, *Nat. Commun.* **2015**, *6*, 5933; b) J. Artz, T. E. Müller, K. Thenert, J. Kleinekorte, R. Meys, A. Sternberg, A. Bardow, W. Leitner, *Chem. Rev.* **2018**, *118*, 434–504.
- [2] M. Aresta, A. Dibenedetto, A. Angelini, *Chem. Rev.* **2014**, *114*, 1709–1742.
- [3] a) S. Inoue, H. Koinuma, T. Tsuruta, *J. Polym. Sci. C* **1969**, *7*, 287–292; b) M. North, R. Pasquale, C. Young, *Green Chem.* **2010**, *12*, 1514–1539; c) P. P. Pescarmona, M. Taherimehr, *Catal. Sci. Technol.* **2012**, *2*, 2169–2187.
- [4] A. J. Kamphuis, F. Picchioni, P. P. Pescarmona, *Green Chem.* **2019**, *21*, 406–448.
- [5] a) J. H. Clements, *Ind. Eng. Chem. Res.* **2003**, *42*, 663–674; b) T. Sakakura, K. Kohno, *Chem. Commun.* **2009**, 1312–1330.
- [6] S. Klaus, M. W. Lehenmeier, C. E. Anderson, B. Rieger, *Coord. Chem. Rev.* **2011**, *255*, 1460–1479.
- [7] C. Martín, G. Fiorani, A. W. Kleij, *ACS Catal.* **2015**, *5*, 1353–1370.
- [8] a) T. Aida, S. Inoue, *J. Am. Chem. Soc.* **1983**, *105*, 1304–1309; b) X. B. Lu, R. He, C. X. Bai, *J. Mol. Catal. A* **2002**, *186*, 1–11; c) C. J. Whiteoak, N. Kielland, V. Laserna, F. Castro-Gómez, E. Martin, E. C. Escudero-Adán, C. Bo, A. W. Kleij, *Chem. Eur. J.* **2014**, *20*, 2264–2275; d) D. O. Meléndez, A. Lara-Sánchez, J. Martínez, X. Wu, A. Otero, J. A. Castro-Osma, M. North, R. S. Rojas, *ChemCatChem* **2018**, *10*, 2271–2277.
- [9] a) D. R. Moore, M. Cheng, E. B. Lobkovsky, G. W. Coates, *J. Am. Chem. Soc.* **2003**, *125*, 11911–11924; b) T. Ema, Y. Miyazaki, S. Koyama, Y. Yano, T. Sakai, *Chem. Commun.* **2012**, 4489–4491.
- [10] R. L. Paddock, Y. Hiyama, J. M. McKay, S. T. Nguyen, *Tetrahedron Lett.* **2004**, *45*, 2023–2026.
- [11] S. Mang, A. I. Cooper, M. E. Colclough, N. Chauhan, A. B. Holmes, *Macromolecules* **2000**, *33*, 303–308.
- [12] For a recent review, see: F. D. Monica, A. Buonerba, C. Capacchione, *Adv. Synth. Catal.* **2019**, *361*, 265–282.
- [13] a) A. Buchard, M. R. Kember, K. G. Sandeman, C. K. Williams, *Chem. Commun.* **2011**, 47, 212–214; b) C. J. Whiteoak, E. Martin, M. M. Belmonte, J. Bene tBuchholz, A. W. Kleij, *Adv. Synth. Catal.* **2012**, *354*, 469–476; c) M. Taherimehr, J. P. C. C. Sertã, A. W. Kleij, C. J. Whiteoak, P. P. Pescarmona, *ChemSusChem* **2015**, *8*, 1034–1042; d) D. Alhashmialameer, J. Collins, K. Hattenhauer, F. M. Kerton, *Catal. Sci. Technol.* **2016**, *6*, 5364–5373; e) F. Chen, N. Liu, B. Dai, *ACS Sustainable Chem. Eng.* **2017**, *5*, 9065–9075; f) M. Cozzolino, V. Leo, C. Tedesco, M. Mazzeo, M. Lamberti, *Dalton Trans.* **2018**, *47*, 13229–13238.
- [14] a) I. Bauer, H.-J. Knölker, *Chem. Rev.* **2015**, *115*, 3170–3387; b) A. Fürstner, *ACS Cent. Sci.* **2016**, *2*, 778–789.
- [15] a) J. E. Dengler, M. W. Lehenmeier, S. Klaus, C. E. Anderson, E. Herdtweck, B. Rieger, *Eur. J. Inorg. Chem.* **2011**, 336–343; b) X. Sheng, L. Qiao, Y. Qin, X. Wang, F. Wang, *Polyhedron* **2014**, *74*, 129–133; c) E. Y. Seong, J. H. Kim, N. H. Kim, K.-H. Ahn, E. J. Kang, *ChemSusChem* **2019**, *12*, 409–415.
- [16] a) M. A. Fuchs, T. A. Zevaco, E. Ember, O. Walter, I. Held, E. Dinjus, M. Döring, *Dalton Trans.* **2013**, *42*, 5322–5329; b) M. Adolph, T. A. Zevaco, C. Altesleben, O. Walter, E. Dinjus, *Dalton Trans.* **2014**, *43*, 3285–3296; c) F. M. Al-Qaisi, M. Nieger, M. L. Kemell, T. J. Repo, *ChemistrySelect* **2016**, *1*, 545–548; d) E. Fazekas, G. S. Nichol, M. P. Shaver, J. A. Garden, *Dalton Trans.* **2018**, *47*, 13106–13112; e) F. D. Monica, B. Maity, T. Pehl, A. Buonerba, A. De Nisi, M. Monari, A. Grassi, B. Rieger, L. Cavallo, C. Capacchione, *ACS Catal.* **2018**, *8*, 6882–6893; f) F. D. Monica, A. Buonerba, V. Paradiso, S. Milione, A. Grassi, C. Capacchione, *Adv. Synth. Catal.* **2019**, *361*, 283–288.
- [17] a) L. Bourget-Merle, M. F. Lappert, J. R. Severn, *Chem. Rev.* **2002**, *102*, 3031–3065; b) R. L. Webster, *Dalton Trans.* **2017**, *46*, 4483–4498.
- [18] a) G. I. Sigeikin, G. N. Lipunova, I. G. Pervova, *Russ. Chem. Rev.* **2006**, *75*, 885–900; b) J. B. Gilroy, M. J. Ferguson, R. McDonald, B. O. Patrick, R. G. Hicks, *Chem. Commun.* **2007**, 126–128; c) M. C. Chang, T. Dann, D. P. Day, M. Lutz, G. G. Wildgoose, E. Otten, *Angew. Chem. Int. Ed.* **2014**, *53*, 4118–4122; *Angew. Chem.* **2014**, *126*, 4202–4206.
- [19] a) R. Travieso-Puente, J. O. P. Broekman, M.-C. Chang, S. Demeshko, F. Meyer, E. Otten, *J. Am. Chem. Soc.* **2016**, *138*, 5503–5506; b) F. Milocco, S. Demeshko, F. Meyer, E. Otten, *Dalton Trans.* **2018**, *47*, 8817–8823.
- [20] a) D. L. J. Broere, B. Q. Mercado, E. Bill, K. M. Lancaster, S. Sproules, P. L. Holland, *Inorg. Chem.* **2018**, *57*, 9580–9591; b) D. L. J. Broere, B. Q. Mercado, J. T. Lukens, A. C. Vilbert, G. Banerjee, H. M. C. Lant, S. H. Lee, E. Bill, S. Sproules, K. M. Lancaster, P. L. Holland, *Chem. Eur. J.* **2018**, *24*, 9417–9425.
- [21] D. L. J. Broere, B. Q. Mercado, P. L. Holland, *Angew. Chem. Int. Ed.* **2018**, *57*, 6507–6511; *Angew. Chem.* **2018**, *130*, 6617–6621.
- [22] R. Travieso-Puente, S. Budzak, J. Chen, P. Stacko, J. T. B. H. Jastrzebski, D. Jacquemin, E. Otten, *J. Am. Chem. Soc.* **2017**, *139*, 3328–3331.
- [23] A. Okuniewski, D. Rosiak, J. Chojnacki, B. Becker, *Polyhedron* **2015**, *90*, 47–57.
- [24] a) J. E. Anderson, C. L. Yao, K. M. Kadish, *J. Am. Chem. Soc.* **1987**, *109*, 1106–1111; b) L. Yu, X. Jin, G. Z. Chen, *J. Electroanal. Chem.* **2013**, *688*, 371–378.
- [25] F. Castro-Gómez, G. Salassa, A. W. Kleij, C. Bo, *Chem. Eur. J.* **2013**, *19*, 6289–6298.
- [26] A. Rehman, A. M. L. Fernández, M. F. M. G. Resul, A. Harvey, *J. CO<sub>2</sub> Util.* **2019**, *29*, 126–133.
- [27] D. J. Darensbourg, J. C. Yarbrough, C. Ortiz, C. C. Fang, *J. Am. Chem. Soc.* **2003**, *125*, 7586–7591.
- [28] J. B. Gilroy, M. J. Ferguson, R. McDonald, B. O. Patrick, R. G. Hicks, *Chem. Commun.* **2007**, 126–128.
- [29] a) H. Tezcan, Ş. Can, R. Tezcan, *Dyes Pigm.* **2002**, *52*, 121–127; b) J. B. Gilroy, S. D. J. McKinnon, B. D. Koivisto, R. G. Hicks, *Org. Lett.* **2007**, *9*, 4837–4840.
- [30] M. C. Chang, E. Otten, *Chem. Commun.* **2014**, *50*, 7431–7433.
- [31] S. D. Ittel, A. D. English, C. A. Tolman, J. P. Jesson, *Inorg. Chim. Acta* **1979**, *33*, 101–106.
- [32] I. G. Ryabokon, O. M. Polumbrik, L. N. Markovskii, *Zh. Org. Khim.* **1983**, *19*, 230–232.

Manuscript received: March 14, 2019  
Revised manuscript received: April 30, 2019  
Accepted manuscript online: April 30, 2019  
Version of record online: July 9, 2019